

7-4-2022

Formation process of underground freshwater based on zoning and stratification of coral reef island

Yuan-jiang JU

School of Resources and Geosciences, China University of Mining and Technology, Xuzhou, Jiangsu 221116, China

Ming-jian HU

State Key Laboratory of Geomechanics and Geotechnical Engineering, Institute of Rock and Soil Mechanics, Chinese Academy of Sciences, Wuhan, Hubei 430071, China, mjhu@whrsm.ac.cn

Yang LIU

School of Resources and Geosciences, China University of Mining and Technology, Xuzhou, Jiangsu 221116, China

Xu ZHU

School of Resources and Geosciences, China University of Mining and Technology, Xuzhou, Jiangsu 221116, China

See next page for additional authors

Follow this and additional works at: <https://rocksoilmech.researchcommons.org/journal>



Part of the [Geotechnical Engineering Commons](#)

Custom Citation

JU Yuan-jiang, HU Ming-jian, LIU Yang, ZHU Xu, QIN Kun-kun, . Formation process of underground freshwater based on zoning and stratification of coral reef island[J]. Rock and Soil Mechanics, 2022, 43(5): 1226-1236.

This Article is brought to you for free and open access by Rock and Soil Mechanics. It has been accepted for inclusion in Rock and Soil Mechanics by an authorized editor of Rock and Soil Mechanics.

Formation process of underground freshwater based on zoning and stratification of coral reef island

Authors

Yuan-jiang JU, Ming-jian HU, Yang LIU, Xu ZHU, and Kun-kun QIN

Formation process of underground freshwater based on zoning and stratification of coral reef island

JU Yuan-jiang^{1,2}, HU Ming-jian¹, LIU Yang², ZHU Xu², QIN Kun-kun²

1. State Key Laboratory of Geomechanics and Geotechnical Engineering, Institute of Rock and Soil Mechanics, Chinese Academy of Sciences, Wuhan, Hubei 430071, China

2. School of Resources and Geosciences, China University of Mining and Technology, Xuzhou, Jiangsu 221116, China

Abstract: In order to understand the significance of stratum stratification characteristics during the formation of underground freshwater lens in the coral reef islands, the particle size distribution (PSD) of the samples drilled at various depths of a coral reef island in the South China Sea is analyzed. The zone and strata of the island are determined according to the PSD characteristics in the horizontal and vertical directions, respectively. The area of each zone is determined based on the range covered by each drilling, and the thickness of each stratum is determined by the thickness of the samples with similar particle size in each drill hole. The permeability of the strata is controlled by the PSD of different zones and strata of the loose layer above the reef limestone, while the vertical and horizontal permeabilities control the difficulty of formation of the underground freshwater lens, the total thickness of the freshwater lens, and the thickness of the transition zone. The numerical model is established by considering the total area of the island and the number of strata. Finally, the numerical results of chloride ion concentration characteristics in the groundwater at different times, horizontal positions and depths are obtained.

Keywords: coral reef island; seawater desalination; zoning and stratification of island

1 Introduction

In recent years, studies have found that on some natural islands far away from the mainland, there are lens-like, thin patches of freshwater formed by rain soaking into the ground, which are well-known as underground freshwater lenses. The underground freshwater lenses formed under natural conditions are valuable and fragile. Their formation and evolution processes are complex, and the amount of freshwater that can be formed is influenced by numerous factors, such as island topographical conditions, hydrogeology, meteorological factors, soil, vegetation and human activities^[1–2].

Coral reef islands are primarily composed of special geomaterials formed by destruction, transportation, accumulation and cementation of the remains of reef-building corals. Calcareous sand is composed of the remains of marine organisms (such as coral, algae and shell) rich in calcium carbonate or other insoluble carbonate substances^[3–5]. The main mineral composition of calcareous sand is the calcium carbonate. During deposition, most of these materials have not been significantly transported and retain the small pores in the protozoa skeleton. Thus the calcareous soil particles are characterized by plenty of internal pores, irregular shapes, weak cementation and high breakability^[6–9].

At present, research on underground freshwater lenses primarily focuses on the freshwater bodies formed in natural islands as well as how to reasonably develop and utilize them. Based on numerical simulations of freshwater development in 36 coral reef islands, Singh

et al.^[10] pointed out that in order to keep the freshwater lens from breaking down, the maximum daily pumping capacity should not exceed 13000 L/d, and the minimum spacing between two pumping wells should not be less than 400 m. Rotzoll et al.^[11] examined the variations in freshwater lens thickness in a basalt island aquifer beneath the coastal sediments for the past 40 years, and found that the thickness of the freshwater lens continues to shrink. This is primarily caused by extraction and irrigation, which make the freshwater lens less sustainable. Zhang et al.^[12] predicted the changes in a freshwater lens under pumping using steady-state analysis. When the pumping rate is 50% of the average water replenishment rate, the maximum thickness of the freshwater lens will be 71% of the average thickness without pumping, and the width of transition zone will increase by 41%. The variation in freshwater lenses during a drought is similar to that under pumping. The depleted freshwater lens takes 1.5 years to recover. Zhao et al.^[3] examined the existence of freshwater lenses on coral reefs in the South China Sea. Fang^[13] examined the Yongxing island, put forward a mathematical model which can reproduce the movement and change law of freshwater lenses in coral reefs by applying the basic theories such as the Darcy's law and the law of conservation of mass, and solved equation discretely.

Most scholars numerically investigated the influences of different factors on the propagation of the transition zone in the lower part of the freshwater lens. For example, Zhou et al.^[14] used GMS software to carry out the numerical simulation of a freshwater lens. According

Received: 14 August 2021

Revised: 25 March 2022

This work was supported by the National Natural Science Foundation of China (41572304, 41877271) and the Strategic Priority Research Program of the Chinese Academy of Sciences (XDA13010301).

First author: JU Yuan-jiang, male, born in 1975, PhD, Associate Professor, mainly engaged in research on landslide debris flow and groundwater dynamics. E-mail: juyuanjiang@cumt.edu.cn

Corresponding author: HU Ming-jian, male, born in 1974, PhD, Research fellow mainly engaged in research on marine geotechnical engineering and landslide and debris flow disasters. E-mail: mjhu@whrsm.ac.cn

to the measured hydrogeological and climatic condition parameters, they analyzed the formation process of the freshwater lens in Yongxing island and established a more realistic and reliable three-dimensional (3D) mathematical model. The numerical results show that the freshwater reserves are the largest in September and the lowest in April, which is consistent with the expectation that the freshwater reserves change with the seasons and rainfall. However, few scholars established the relationship between the formation of freshwater lenses and stratigraphic characteristics, while the stratigraphic characteristics have significantly impact on the formation of freshwater lens.

Based on previous research, the complete formation process of a coral reef island is analyzed through field drilling experiments, and the influence of freshwater lens formation on the coral reef island with elapsed time is numerically investigated. Also, the time required for the freshwater lens to reach stability is predicted, which is of great significance to the subsequent development of freshwater lens body.

2 Stratigraphic and climatic characteristics of typical coral reef islands

2.1 Stratigraphic characteristics

The Nansha Islands and the adjacent sea areas are located in the southern region of the South China Sea, near the intersection of the Eurasian Plate, Indo-Australian Plate and Pacific Plate. The formation and development of the geological structures in this area are affected and controlled by aforementioned three plates. In the long geological history, strong magmatic activity and frequent tectonic movement produced different strata and rocks and developed complex topographic features, which formed the geological structural basis of seabed and land in this area, and created conditions for the source of seabed sediments. A coral reef is a raised terrain formed on the seabed, extending from the seabed to the sea surface, which is discontinuous with the surrounding rock strata. Because the coral cannot grow above the water surface, it can only expand under the water surface based on the sea level. Therefore, all reefs have large reef plates, which are reef platforms formed at the top of the reef at sea level. The coral around the platform grows fast and rises slightly, which is conducive to the accumulation of coral fragments and biological debris, resulting in a dish-shaped reef platform which is low inside and high outside. When the deposits on the reef rise above sea level, they form sandbars and further evolve into coral islands^[14].

The coral reefs are porous and stratified, and these features are dependent upon the formation and accumulation process of coral reefs. The coral reef islands are formed by accumulation or cementation diagenesis of coral reef fragments, gravel and shells. The surface layer of the coral reef island forms relatively late and is composed of loose, unconsolidated, or weakly cemented coral and bioclastic materials. Below the surface layer, there are ancient alternating, petrochemical and diagenetic

coral reef limestone and coral shell limestone. Due to different sizes and shapes of reef blocks in coral reef islands, the loose sediments have various types of pores, resulting in different pore distributions in the upper and lower layers of the island. Generally speaking, the surface layer containing small pores is classified as low-permeability stratum. The lower coral reef limestone is seriously eroded, and the karst caves and pores are well developed, thus this layer is classified as high-permeability stratum^[15].

In this paper, a coral reef island in the South China Sea was selected. In order to study the shallow strata characteristics of the coral reef island in detail, core extraction was carried out for the complete drilling section of each borehole, including the loose strata from the surface to the top of the reef limestone layer. Particle size distribution (PSD) characteristics were visually inspected in the field to preliminarily acquire the stratigraphic information. In order to further determine the stratification characteristics, the boundary at the obvious variation of the PSD was marked and the representative soil samples were taken for laboratory particle analysis.

According to the core characteristics, the calcareous sand strata, especially the shallow part, are discontinuous, while the boundary between reef limestone and overlying loose layer is clearly visible. The reef limestone is generally composed of hard rock blocks with calcareous cement. Obvious corroded grooves can be observed on the core surface, and they account for more than 30% of the total area. The maximum inner diameter and extension length of grooves and corroded holes both can reach more than 30 mm. The reef limestone strata must have experienced a significant sedimentary discontinuity during the Quaternary, resulting in strong karst formation. The large number of pores and caves make the permeability of the reef limestone strata generally greater than 500 m/d.

Most of the original reef flats under the islands and reefs are exposed above the sea level at low tide and submerged at high tide. The tidal range is 1.5 m, and the surface is approximately 4 m above the high tide level after hydraulic reclamation. The average depth of the hydraulic reclamation interface is about 5.5 m. At this depth, each borehole generally contains fine sand, medium sand and gravel sand. Also, a small amount of gravels can be observed in some boreholes. The dredger material comes from the lagoon on the east side of the original reef flat. Due to the poor hydrodynamic conditions of the lagoon, the sediment particles are relatively fine, and the particles in the dredger fill layers are primarily relatively fine. The underlying loose layer on original reef flat composed of naturally deposited sediments is relatively continuous, but it is difficult to accurately distinguish the boundary between the dredger fill layer and the original loose layer. The internal strata of the island can be divided in transverse and longitudinal directions, and the corresponding stratigraphic distributions are shown in Tables 1 and 2.

Table 1 Transverse stratigraphic characteristics of the island

Borehole number	Thickness /m	Stratum
JC503	0.0–2.0	Medium sand
	2.0–6.18	Gravelly sand
	6.18–16.5	Breccia
	16.5–21.7	Gravelly sand
ZK509	0.0–2.6	Gravelly sand
	2.6–3.4	Fine sand
	3.4–9.1	Medium sand
	9.1–14.8	Gravelly sand
	14.76–23.1	Breccia
ZK503	0.0–6.6	Gravelly sand
	6.6–12.5	Breccia
	12.15–21.73	Crushed stone

Table 2 Longitudinal stratigraphic characteristics of the island

Borehole number	Thickness /m	Stratum
JC504	0.0–4.5	Medium sand
	4.5–5.8	Fine sand
	5.8–10.8	Medium sand
	10.8–15.2	Fine sand
	15.2–19.7	Gravelly sand
ZK509	0.0–2.6	Gravelly sand
	2.6–3.4	Fine sand
	3.4–9.1	Medium sand
	9.1–4.8	Gravelly sand
	14.76–23.1	Breccia
ZK501	0.0–3.3	Gravelly sand
	3.3–5.0	Breccia
	5.0–5.4	Fine sand
	5.4–12.4	Gravelly sand
	12.4–15.0	Fine sand
	15.0–24.71	Gravelly sand

From the top surface of the continuous reef limestone layer to the surface of the island, the borehole cores are primarily composed of loose sand, gravel sand and crushed stone. In general, the shallow island sediments are fine and the deep sediments are coarse, and its boundary is located at the depth between 4.3 m and 7.3 m.

2.2 Strata permeability characteristics

In order to further understand the PSD characteristics of the shallow soil layer of the coral reef island, the loose strata between the current island surface and the top surface of the continuous reef limestone were discriminated and analyzed in detail. The core samples were placed in order according to the footage sequence on the label, the PSD characteristics were observed, and preliminary segmentation was conducted by means of visual measurement and hand contact. All the clearly visible changes in particle size composition, soil color, as well as the characteristics of biological fragments in the soil were marked as the suspected particle size change interface, and the corresponding interface depths were recorded. A certain amount of representative soil samples were taken from all of the suspected particle size change sections for laboratory particle analysis tests, in order to further verify and determine the PSD characteristics at different depths. The final PSD was classified following the classification standard for sand in the *Code for Investigation of Geotechnical Engineering* (GB 50021–2001)^[16]. According to the PSD curve, the sizes of the particle corresponding to 10%, 30% and 60% finer (d_{10} , d_{30} and d_{60}) of the soil samples in each layer were determined, and the coefficient of uniformity

C_u and the coefficient of curvature C_c were calculated. If the names of adjacent layers are the same, and the values of d_{10} , d_{30} , d_{60} , C_u and C_c obtained from the PSD are similar, the two layers should be merged. Permeability tests were carried out, and the specific permeability coefficients are shown in Table 3.

Table 3 Statistics of permeability coefficient of calcareous sand

Data sources	Soil sample	Value range /($\text{cm} \cdot \text{s}^{-1}$)	Representative value /($\text{cm} \cdot \text{s}^{-1}$)
Measured data	Fine sand	$4.1 \times 10^{-4} - 2.6 \times 10^{-3}$	1.45×10^{-3}
Measured data	Medium sand	$1.6 \times 10^{-3} - 4.2 \times 10^{-3}$	1.64×10^{-3}
Zhu ^[17]	Coarse sand	$3.6 \times 10^{-3} - 1.0 \times 10^{-2}$	4.30×10^{-3}
Measured data	Gravelly sand	$4.8 \times 10^{-3} - 5.3 \times 10^{-2}$	2.60×10^{-2}
Measured data	Breccia	$2.1 \times 10^{-1} - 5.0 \times 10^0$	1.47×10^{-1}
Zhu ^[17]	Crushed stone	$1.0 \times 10^0 - 1.0 \times 10^1$	1.00×10^0

2.3 Climatic characteristics

The Nansha Islands and the adjacent coastal area are sunny, moist, and have abundant rainfall under the monsoon tropical marine climate. The average temperature is 27.84 °C. The lowest monthly average temperature occurs in January, and the highest one occurs in late May. The annual average relative humidity is 86%. The annual rainfall has an uneven geographical distribution, and the number of annual rainy days can generally exceed 130 d. The rainfall occurs primarily during the southwest monsoon period, while rainstorm and extraordinary rainstorm are primarily concentrated from July to September. The surface water of the Nansha Islands and the adjacent sea area are one of the highest temperature waters in the world (commonly around 30 °C and even above 31 °C in the southern continental shelf). Even in winter, the surface water temperature is greater than 28 °C. The surface water temperature is greater than the average sea surface temperature of whole year, especially in winter^[18].

The year-round high temperature provides the conditions for a large amount of evaporation of sea water. The evaporated water can easily form rainfall after rising and cooling. Seasonal variations in rainfall on coral reefs have an important impact on the supply and consumption of freshwater lenses. In order to simulate the infiltration issue under rainfall–evaporation conditions, it is essential to analyze the rainfall–evaporation conditions of coral reef islands. Meteorological data for the South China Sea were collected, and the rainfall and evaporation data from September 2017 to August 2018 were analyzed.

Assuming a monthly rainfall greater than 100 mm for the rainy season, and a monthly rainfall less than 100 mm as dry season, February, March, April and May are classified as the dry season, and January, June, July, August, September, October, November and December are the rainy season. The annual cumulative rainfall is 2 355.4 mm, the annual average daily rainfall is 7.1 mm, the maximum daily rainfall is 116 mm, and the minimum daily rainfall is 0 mm. The lowest daily evaporation value of the whole year is from April to June, during which the daily accumulated evaporation capacity is much lower than that of other months, which is almost

zero. The daily evaporation capacity in other months is relatively high and stable, most of which is approximately 6 mm. The daily cumulative evaporation capacity of the whole year is 1593.5 mm, and the daily average evaporation capacity of the whole year is 4.7 mm.

3 Mechanism of groundwater desalination

3.1 Constitutive equation

For the coral reef, water flow in the freshwater lens is a 3D motion coupled with variable density flow and solute transport. This kind of flow problem is described by two partial differential equations. One is used to describe the variable density flow, and the other is used to describe the solute motion in the fluid. Therefore, when establishing the 3D mathematical model for the freshwater lens, the conventional dynamic equation needs to be modified to consider the influence of density change on flow motion^[19]. The law of conservation of mass and the Darcy's law are the theoretical bases for constructing a 3D mathematical model. Different from two-dimensional model, the influence of solute density on water head should be considered.

The mathematical model of the coral reef island is a 3D variable density groundwater flow model, in which the governing equation for the 3D variable density flow is

$$\frac{\partial}{\partial \alpha} \left[\rho K_{f\alpha} \left(\frac{\partial h_f}{\partial \alpha} + \frac{\rho - \rho_f}{\rho_f} \frac{\partial z}{\partial \alpha} \right) \right] + \frac{\partial}{\partial \beta} \left[\rho K_{f\beta} \left(\frac{\partial h_f}{\partial \beta} + \frac{\rho - \rho_f}{\rho_f} \frac{\partial z}{\partial \beta} \right) \right] + \frac{\partial}{\partial \gamma} \left[\rho K_{f\gamma} \left(\frac{\partial h_f}{\partial \gamma} + \frac{\rho - \rho_f}{\rho_f} \frac{\partial z}{\partial \gamma} \right) \right] = \rho S_f \frac{\partial h_f}{\partial t} + \theta \frac{\partial \rho}{\partial c} \frac{\partial c}{\partial t} - \bar{\rho} q_s \quad (1)$$

where h_f is the equivalent head of freshwater; K_f is the permeability coefficient (with freshwater as reference); S_f is the water storage rate (with freshwater as reference); θ is the effective porosity; ρ is the density of the mixed fluid; ρ_f is the density of freshwater; q_s is the flow rate of source (or sink) per unit volume of porous media; $\bar{\rho}$ is the density of the source (or sink); $K_{f\alpha}$, $K_{f\beta}$ and $K_{f\gamma}$ are the components of the permeability coefficients in α , β and γ directions, respectively; c is the solute concentration; and t is the time.

The governing equation for the solute transport is

$$\frac{\partial C}{\partial t} = \nabla \cdot (\mathbf{D} \cdot \nabla C) - \nabla \cdot (VC) - \frac{q_s}{\theta} C_s + \sum_{k=1}^N \mathbf{R}_k \quad (2)$$

where \mathbf{D} is the hydrodynamic dispersion coefficient tensor; V is the average flow velocity of groundwater; C_s is the concentration of source (or sink) fluid; \mathbf{R}_k is the chemical reaction term; and C is the solute concentration.

After establishing the mathematical model, in principle, the conventional analytical method can be used to solve the continuous function satisfying the governing equation as well as the conditions of a definite solution, in order to determine the parameters such as water head at any point and any time in the

freshwater lens body. The analytical method can accurately obtain the calculation results, the calculation steps are simple, the physical concept of the calculation formula is clear, and it is easy to analyze the influence of various factors on the freshwater lens. However, the analytical method is only suitable for isotropic aquifers with a simple equation and regular aquifer shape. In practical application, there are few cases which can satisfy these conditions, and thus most cases are solved using numerical methods.

3.2 Hydrodynamic dispersion

Hydrodynamic dispersion includes mechanical dispersion and molecular diffusion of a solute in porous media. Both the velocity and the direction of liquid motion vary, which is primarily related to the viscosity of the liquid and the frictional resistance of combined water to gravity water, as well as the fact that the flow velocity near the pore wall approaches zero and gradually increases to the maximum at the pore center. Pore size variations result in differences in maximum axial velocity between different pores. If the pore itself is crooked, the direction of the water flow is constantly changing. Therefore, for the average direction of the water flow, the position of the specific streamline swings in space. These phenomena occur simultaneously, resulting in the tracer particles, which are close to each other at the beginning of the flow process, not always moving according to the average velocity, but continue to expand around, beyond the expected range of expansion based on the average velocity, which can be observed along the direction of average velocity and perpendicular to it. When the liquid flows through porous media, material migration caused by uneven velocity is called mechanical dispersion. Molecular diffusion is a kind of material migration caused by an uneven concentration of solute in liquid. The concentration gradient makes the substance move from high concentration areas to low concentration areas, causing the overall concentration more uniform. Molecular diffusion can also occur in stationary liquids and makes the concentration in the same first-class beam uniform. There is also material exchange between adjacent flow beams due to the concentration gradient, which leads to a decreasing transverse concentration difference.

When liquid flows in porous media, mechanical dispersion and molecular diffusion occur simultaneously and they are inseparable. When the velocity is high, mechanical dispersion is the primary factor. When the flow rate is small, the effect of molecular diffusion becomes significant. Both mechanical dispersion and molecular diffusion can make a solute expand both along the average flow direction and perpendicular to it. The former is called longitudinal dispersion, and the latter is called transverse dispersion^[20].

4 Numerical simulation of groundwater desalination process

4.1 Model condition setting

Visual MODFLOW was used to simulate the groundwater desalination process using a 3D mathematical model

considering the variable density groundwater and solute transport in a coral reef island. In this simulation, the coral reef island is 4 m above the sea level and the reef limestone is 25 m below the ground. The development range for the freshwater lens of the island cannot enter the reef limestone. In order to ensure the accuracy of the model simulation and reduce calculation workload, this model sets the base level at 30 m below the ground level of the coral reef island and establishes a 3D rectangular coordinate system with the origin on the datum plane.

The lengths of the long and short axes are 3.7 km and 1 km, respectively. The average altitude of the island is 4 m, and the terrain is flat. The original lagoon water depth ranges between 25 m and 30 m. Eight boreholes were arranged on the island in three survey lines along the long axis of the island. In order to well show the simulation results, the coral reef island extends appropriately along the length and width below the sea level. The whole model is about 3720 m long, 3120 m wide and 30 m high. The thickness of the portion of the model above sea level is 4 m, and that below sea level is 26 m.

The simulation object is the salt displacement in calcareous sand with a relatively large permeability coefficient. Theoretically, both convection diffusion and molecular diffusion control the salt migration process. Zhou et al.^[14] pointed out that for the groundwater and solute transport in coarse-grained soil, the influence of convection diffusion is dominant and much greater than that of molecular diffusion. Therefore, when considering the salt transport process, the convection diffusion process under the influence of permeability coefficient is taken as the primary mechanism, and molecular diffusion is treated as constant. The simulated solute has a single component, and there is no mature theory or mathematical model for analyzing the salt desorption and readsorption process of calcareous sand, thus a non-adsorption simulation is used in this study. Meanwhile, the primary solute component in seawater is NaCl, which has a good chemical stability and does not produce chemical reactions that can lead to salt variation in calcareous sand formation. Therefore, the chemical reaction is also neglected in this solute transport simulation.

The mesh generation of the model includes plane mesh generation and vertical layered generation. The basic mechanism of freshwater conservation in coral reef islands is that the groundwater is displaced by rainwater infiltration. Therefore, the effect of groundwater vertical seepage to a certain depth cannot be ignored. This process is controlled by the vertical convection diffusion, while the convection diffusion is subjected to the permeability coefficient. The vertical divisions of this model should be much finer than other models. The total strata thickness in this simulation is 30 m, and the size of each layer is 0.5 m. In this paper, borehole data are adopted for zoning, and taking the

center line of adjacent boreholes as boundaries, the whole model is divided into eight areas. The permeability coefficient of the corresponding layer is used as the representative value of the area. Therefore, permeability coefficients vary in different areas and at different depths.

Before reclamation, most of the simulated coral reef islands are located below sea level. After reclamation, cofferdams are set around the islands to stabilize the reclamation strata. The role of cofferdams also includes limiting the horizontal seepage of groundwater above sea level and acting as a horizontal impermeable boundary for strata above sea level.

All the grids except the coral reef island are set as invalid grids and do not participate in the simulation process. For the strata below sea level, the horizontal expansion is approximately 10% of the island length on each side, which can accurately simulate the groundwater of the whole island without significant excess calculation. The northern port and southeastern small lagoon are occupied by seawater; therefore, the groundwater seepage cannot pass through. These locations are discharge boundaries for groundwater in essence, and are also set as invalid grids. To summarize, the model is divided into 132 columns and 130 rows on the partition plane, with row spacing by column spacing of 30 m×30 m. In the vertical direction, the model is divided into 60 layers with a 0.5 m-thickness for each layer. There are 8 layers above sea level and 52 layers below sea level. For the portion above sea level, the scope of the coral reef island is drawn based on the base map of the coral reef island. For the portion below sea level, based on the original scope of the coral reef island, the scope of the model participating in the simulation is expanded according to the above expansion principle.

The simulation primarily shows the state of coral reef island at the characteristic time point by means of the change in NaCl concentration in groundwater. Therefore, the output concentration state is recorded at 365 d (1 year), 1825 d (5 years), 3650 d (10 years) and 7300 d (20 years), respectively. In order to clearly describe the groundwater conservation process, data and images for different locations, times and parameters are extracted from the simulation results file for comparative analysis. The selected position is determined according to the key horizontal section, transverse section and longitudinal section. The freshwater generation process in this simulation can be represented by the change in solute concentration; therefore, chloride ion concentration is the desired parameter. Based on the geological model described above, the parameters change significantly at the early stage of seepage but vary slightly at the later stage. Therefore, the simulation results are displayed with high density at the early stage and with low density at the later stage. The chloride ion concentration at each position is analyzed after 1 year, 5 years, 10 years and 20 years.

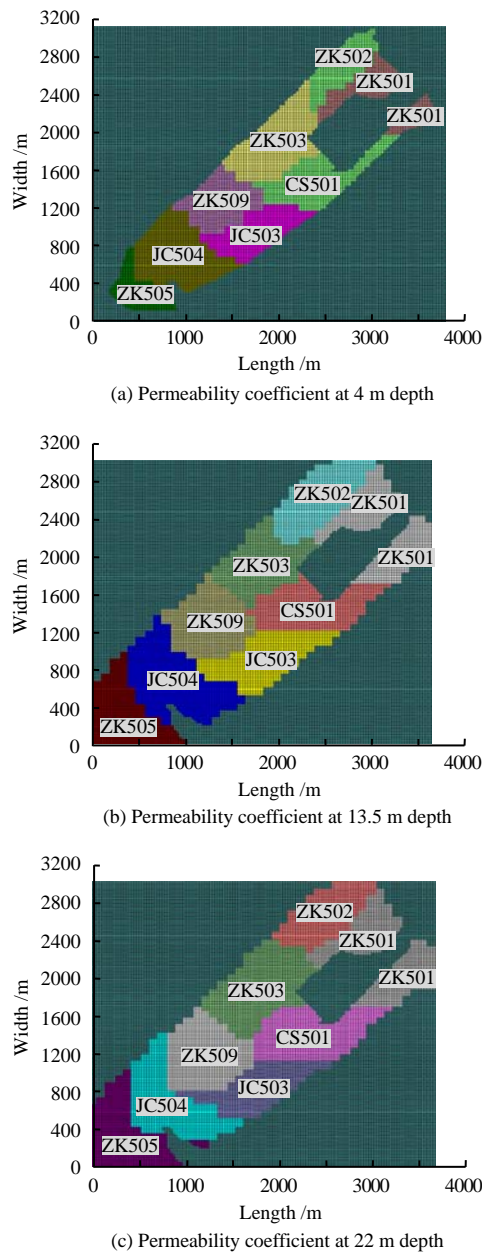


Fig. 1 Assignment of permeability coefficient at each depth

4.2 Desalination process at different depths

Due to the lack of horizontal seepage above sea level, vertical seepage can displace saline groundwater more effectively, and the desalination process is simpler and more efficient than groundwater seepage below sea level. Due to the lack of a cofferdam and influenced by the tidal process, the horizontal seepage of ground-water begins to occur near sea level.

In the first year, the concentration changes slightly at 4 m depth (Fig.2(a)). The concentration at the northwest, mid-north and mid-east of the island is 1000–3000 mg/L, and the concentration at the north, mid-west and south of the island is 3000–5000 mg/L. Brine stripes with a chloride ion concentration greater than 10000 mg/L are found near the center of the island. There are no areas with a chloride ion concentration less than 1000 mg/L at 4 m depth in the first year. At the fifth year, except for the narrow terrain in the north and the arc-shaped stripe in the center of the island, the concentration drops to less than 1000 mg/L (Fig.2(b)).

From the 10th year to the 20th year, the high concentration area in the north and central arc stripes decreases and even disappears (Fig.2(c) and (d)), and the whole layer is completely desalinated in the 10th year.

Most of the strata near the sea level are hydraulically filled, and part of original reef flat strata exists. Reef limestone is located 20 m below sea level. The strata below the sea level and above the reef limestone are primarily original reef flat strata, which were formed in the late Pleistocene and Holocene with a loose structure. The PSD characteristics are primarily determined by the hydrodynamic conditions during the Quaternary period. Due to significant changes in the hydrodynamic conditions near the reef flat, such as waves and storm surges, the PSD characteristics and permeability of this part of the strata vary in both horizontal and vertical directions. The middle of this part of strata is the primary research target, and the groundwater chloride ion concentration at 13.5 m depth is taken as the index to analyze the groundwater desalination process in the middle of the original loose strata.

By comparing the concentration diagram for each year, it is found that after one year of rainwater infiltration, the salt displacement process occurs in the 27th layer at 13.5 m depth, and the change range is greater at the south of the island. Also, the area with a concentration of 8000–15000 mg/L is presented, but the whole layer of groundwater is still saline (Fig.3(a)). In the 5th year, the areas with a concentration less than 1000 mg/L are found at the mid-west of the island and the west of the port (Fig.3(b)). After the 10th year, the areas with a concentration less than 600 mg/L are presented on the mid-north and mid-west of the island, the north of the lagoon, and the west of the port. There is a triangle area with concentration of 1000 mg/L in the northwest of the middle part, and the concentration in other areas is less than 1000 mg/L (Fig.3(c)). Compared to the concentration diagram at 4 m depth (Fig.2), the concentration change at 13.5 m depth is not only limited to the inside of the island but also occurs in the external expansion part of the island. In the 20th year, the groundwater in the island further desalinates, and the triangular area with a concentration of more than 1000 mg/L in the northwest and central areas still exists, indicating that the freshwater lens could reach 13.5 m below ground level. However, some areas could not be completely desalinated and are still in the transitional zone.

At 22 m depth, most of the boreholes enter the reef limestone strata, which can represent the furthest extension of the freshwater lens. Therefore, the change in chloride ion concentration with time at 22 m depth is analyzed.

Through analyzing the chloride ion concentration diagram of the island at the first year (Fig.4(a)), the concentration of the whole layer remains in a relatively high concentration range and basically keeps unchanged, indicating that one year's duration is not enough to cause a significant concentration change at 22 m depth. Between the first and fifth years, the whole island enters a high concentration state. During the fifth year, a small triangular area with a concentration less than 1000 mg/L appears at the mid-south of the island (Fig.4(b)).

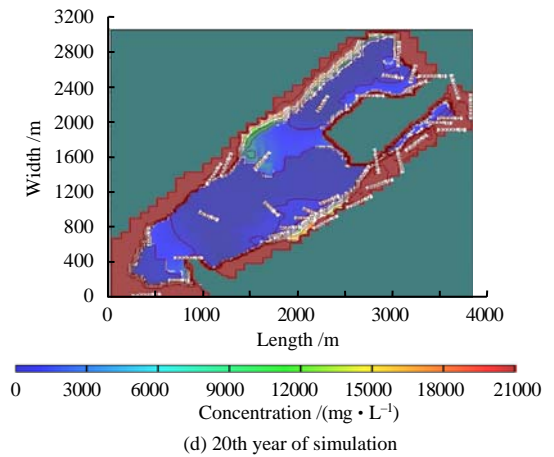
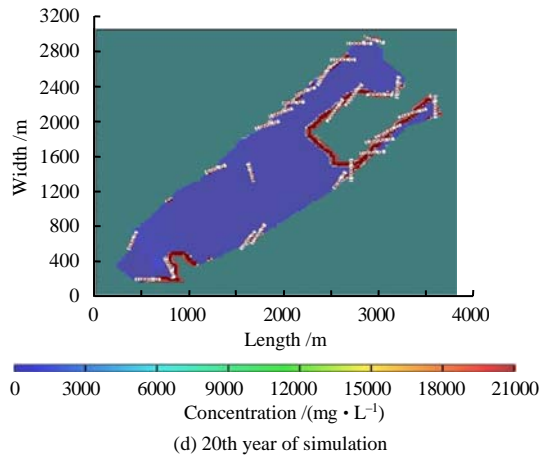
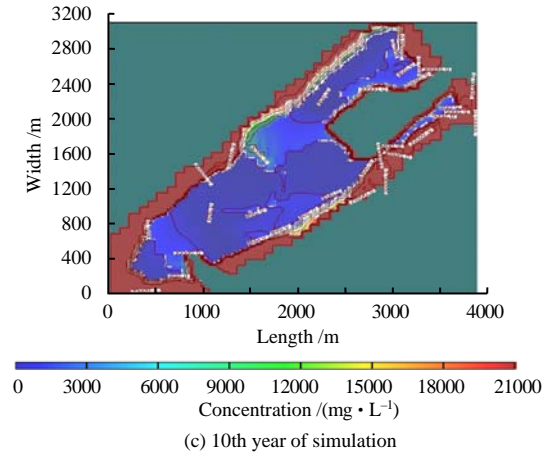
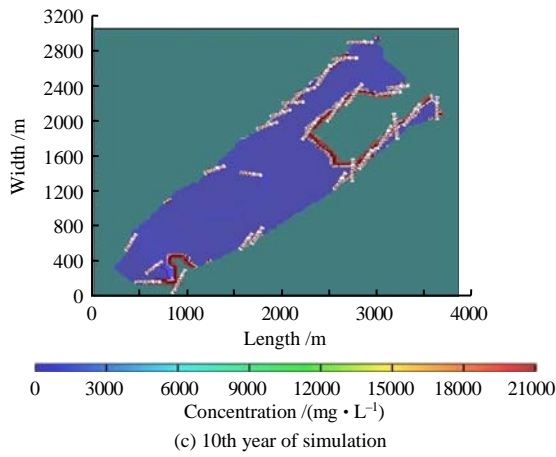
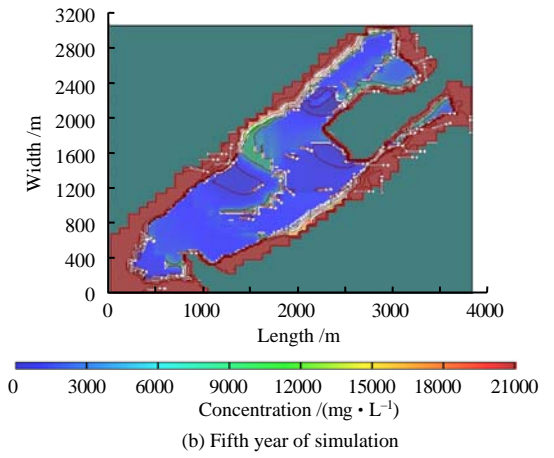
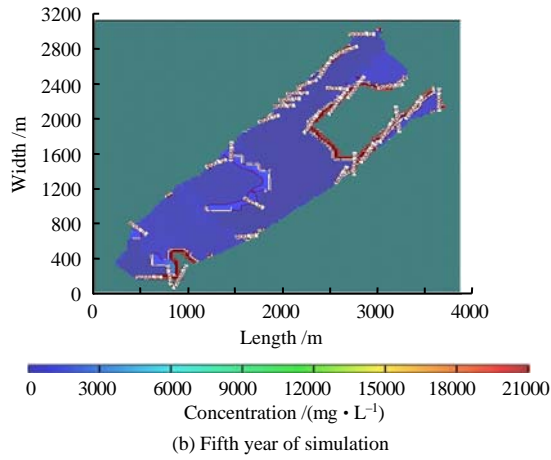
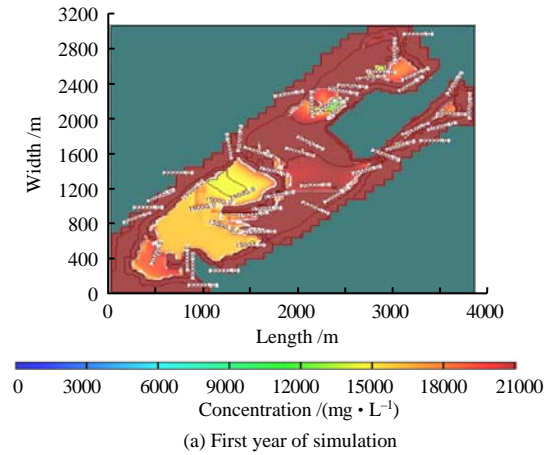
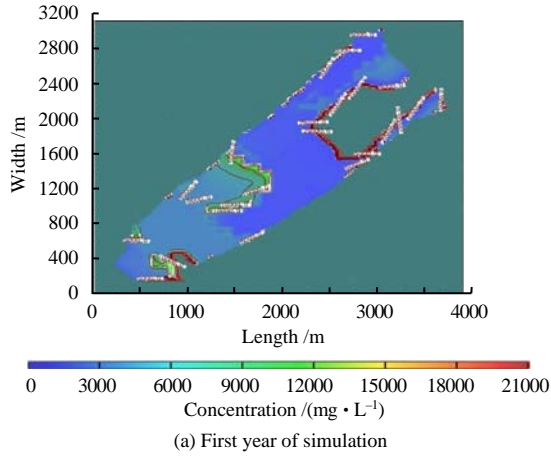


Fig. 2 Annual concentration diagrams at the depth of 4 m

Fig. 3 Annual concentration diagrams at the depth of 13.5 m

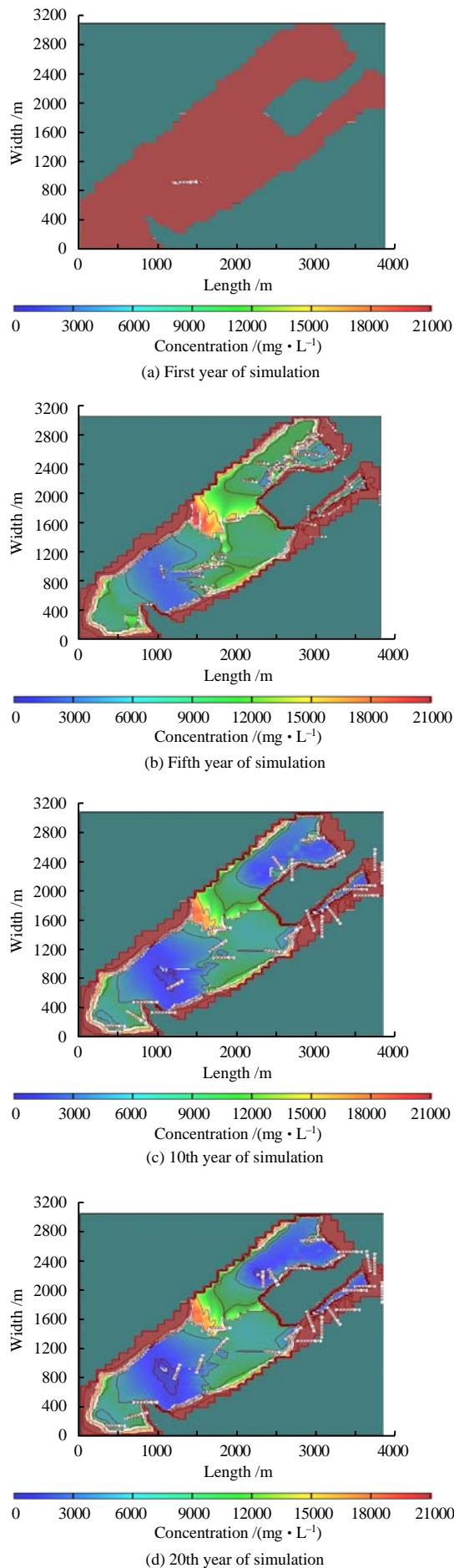


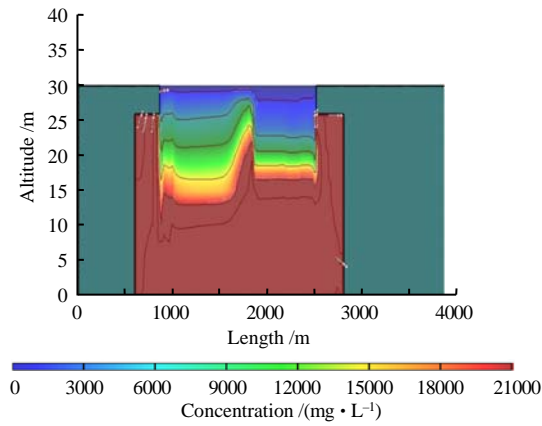
Fig.4 Annual concentration diagrams at the depth of 22 m

As shown in Fig.4(c), at the 10th year, the small triangular area at the mid-south of the island further desalinates and the desalination range increases, while the concentration at the west of the port is less than 1000 mg/L. As shown in Fig.4(d), in the 20th year, all areas of the island are desalinated slightly, but in most areas except the mid-south of the island and the west of the port, the concentration remains above 5000 mg/L. In the areas with higher desalination degree, the permeability coefficient of the shallow strata is smaller, and more freshwater can be retained in the strata. Freshwater can also infiltrate into the reef limestone at this depth. However, the permeability coefficient of the reef limestone is too large, and the reef limestone strata can be quickly occupied by underground water due to a short-term rise in sea level during the tidal process. Therefore, groundwater desalination in the reef limestone is quite active, which is theoretically meaningless to the ecology of artificial coral reef islands and the development of freshwater on the island. This observation also shows that the above geological model is reasonable to consider the top boundary of reef limestone as the bottom boundary of freshwater lens development.

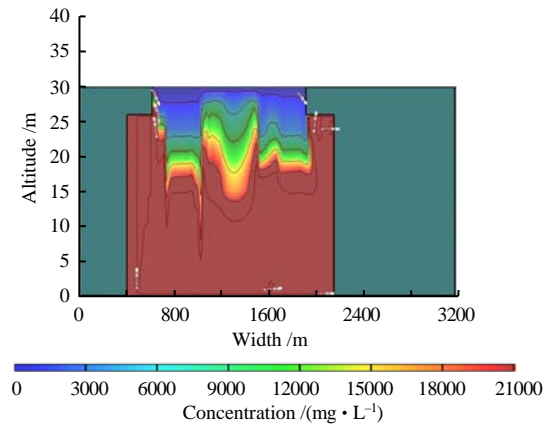
4.3 Desalination process at different horizontal positions

Figures 5 and 6 respectively show the transverse and longitudinal sections of the middle of the island to better illustrate the concentration variation. The transverse section is located in the middle of the island. At this location, the shallow strata are primarily composed of medium sand and gravel sand, while the deep strata are primarily composed of gravel sand and breccia. Compared with the north of the island, the permeability in the middle is relatively poor.

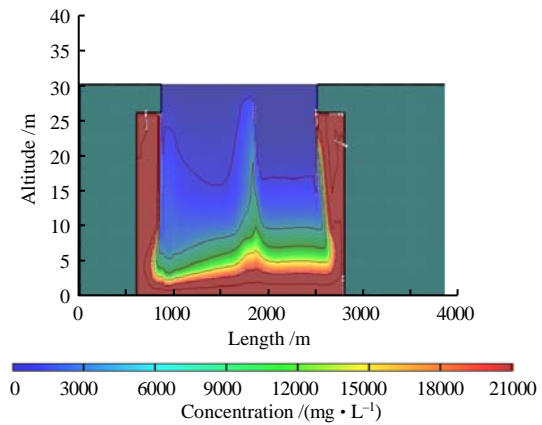
As shown in Fig.5(a), in the first year, the concentration changes significantly above sea level, and the concentration in the eastern area is significantly lower than that in the western area. The permeability coefficient of the strata in the east is slightly larger than that in the west, which will lead to the infiltration of freshwater and faster salt displacement in the east. In the western area, the rainwater infiltration is slower compared to that in the eastern area because the permeability coefficient of strata is smaller. However, the large permeability coefficient also makes the rainwater in the eastern area more difficult to retain compared to the western area. During rainwater infiltration, rainwater is difficult to exist in the strata and quickly converge into the sea water. Because of the small permeability coefficient in the western area, freshwater can be kept in the strata, and thus the depth of desalination can be greater. Compared with the 5th year, the concentration of freshwater in the 10th year changes significantly (Fig.5(b)). The development depth of freshwater in the western area is significantly greater than that in the eastern area. After the 10th year, the concentration of freshwater primarily changes in the center. Also, the eastern and western areas basically reach a stable state with almost no change (Fig.5(c)). After 20 years of desalination, the maximum depth of the freshwater line in the western



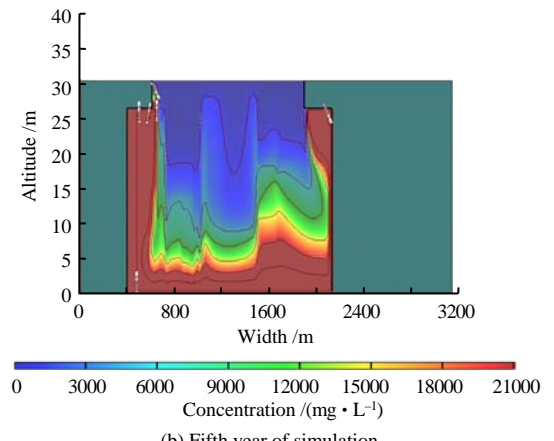
(a) First year of simulation



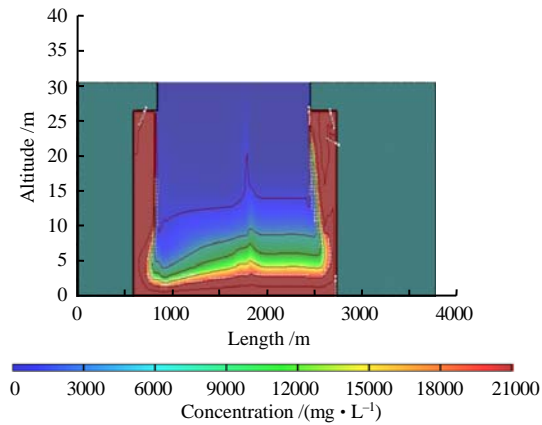
(a) First year of simulation



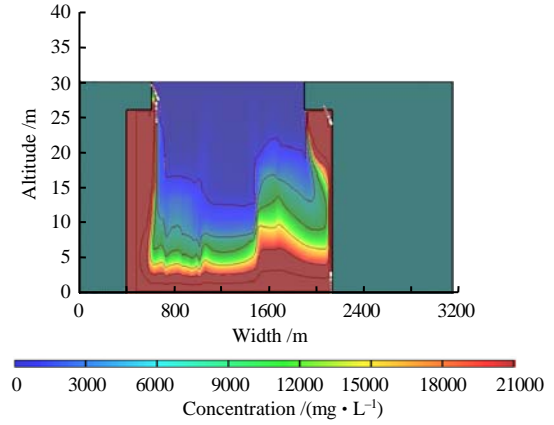
(b) Fifth year of simulation



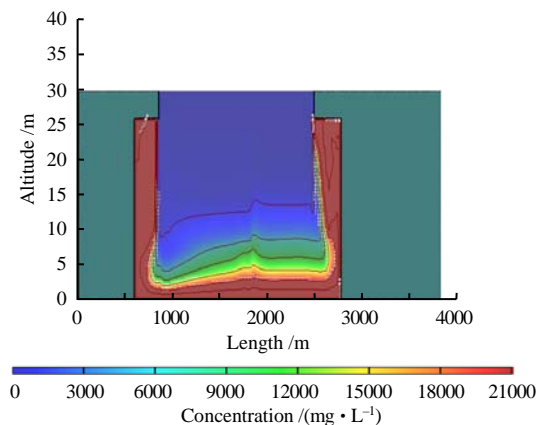
(b) Fifth year of simulation



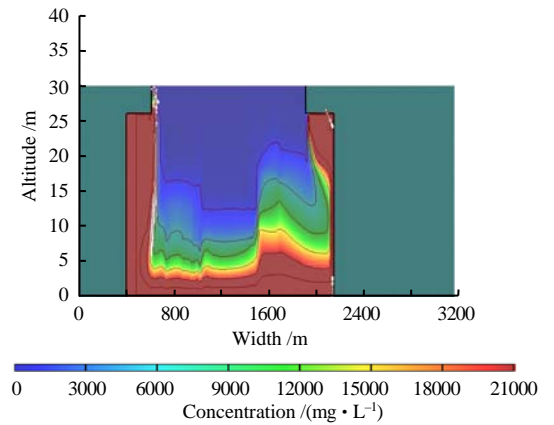
(c) 10th year of simulation



(c) 10th year of simulation



(d) 20th year of simulation



(d) 20th year of simulation

Fig. 5 Annual concentration diagrams of transverse section in the middle of coral reef island

Fig. 6 Annual concentration diagrams of longitudinal section in the middle of coral reef island

area is approximately 22 m below the ground, while that in the eastern area is approximately 20 m. The transition zone on both the east and west sides have a proper outward expansion. The western area begins to expand at the position 18 m below the ground, and the eastern area begins to expand at the position 10 m below the ground. The thickness of the transition zone on both east and west sides is 6–8 m (Fig.5(d)).

The longitudinal profile is located in the middle part of the whole artificial coral reef island and can show the variation in groundwater concentration in the middle part of the island. The strata in the middle area are complex. The permeability coefficient varies significantly from north to south, and the profile can be divided into three parts, corresponding to the strata in the north, middle and south. The shallow northern strata primarily contain gravel sand, and the deep strata are composed of breccia with high permeability coefficient. The southern strata are primarily composed of gravelly sand and breccia, and the permeability coefficient is also large. The strata in the middle are composed of fine sand and medium sand with breccia in the deep part, and the permeability coefficient is less than that in the north and south.

As shown in Figs.6(a) and (b), from the first year to the fifth year, the advancing speed of desalination on the north and south sides is much faster than that in the middle. In the fifth year, the 600 mg/L concentration line on the south side will progress to 8 m below the ground, the 600 mg/L concentration line on the north side will progress to 6 m below the ground, and the 600 mg/L concentration line in the middle is located at the depth less than 3 m. The permeability coefficient of the middle strata is small, and the rainwater cannot easily infiltrate. Therefore, in the first few years, the concentration of groundwater at this position will be maintained at a high level, while the seepage speed of groundwater in the south and north is fast and the drainage path is short, allowing the low concentration area to extend into the deeper strata. From the 5th year to the 10th year, the depth of the low concentration area in the middle can exceed that in the north and south. After 20 years of desalination, the desalination degree in the middle is the best, and the maximum depth of the waterline is about 20 m below the ground (Figs.6(c) and (d)). The desalination degree of the southern region is the second best, and the maximum depth of the waterline is about 14 m below the ground. The desalination degree of the northern region is the worst, and the maximum depth of its waterline can only advance to approximately 10 m below the ground. The maximum thickness of the transition zone in the central region is approximately 6 m on the north and south sides, which is thicker than that in the central region. At the position where the permeability coefficient is larger, the freshwater line is shallower, and the transition zone is thicker. At the position where the permeability coefficient is smaller, the freshwater line is deeper, and the transition zone is thinner, which is consistent with the theoretical derivation of the previous geological model.

5 Conclusions

The thickness of a fresh groundwater aquifer is related to the length of the groundwater infiltration path. In the middle part of a coral reef island, the vertical component of groundwater seepage is large, the seepage path is long, and the freshwater layer is relatively thick. The horizontal component of groundwater seepage around the island is large, the seepage path is short, the freshwater layer is relatively thin, and the freshwater layer is lens-shaped in profile. The freshwater lens thickness is related to the permeability of formation and decreases with increasing permeability.

The thickness of the transition zone between the freshwater line and saltwater line is related to the permeability and length of the seepage path. A larger permeability results in a thicker transition zone, and a longer seepage path results in a thinner transition zone. The freshwater lens cannot be formed in the narrow terrain above sea level, the amount of freshwater supplied by rainfall is small, and the groundwater discharge path is short.

The freshwater line below sea level can extend beyond the island borderline. The wide expansion range is generally induced by the thick freshwater lens, the small formation permeability, the wide terrain above the sea level, and the farther distance from the underground water discharge boundary. The speed of groundwater desalination is related to the length of infiltration path, strata permeability and desalination stage. The longer the infiltration path is, the slower the freshwater line advances. At the early stage of desalination, the larger the permeability is, the faster the freshwater line advances. At the middle and late stages of desalination, the larger the permeability is, the easier the waterline reaches a stable position.

The freshwater lens of a coral reef island can only form in a relatively loose environment. Reef limestone contains corroded holes and pores which cannot retain freshwater. Twenty years after the completion of hydraulic reclamation, the freshwater line will be close to the upper boundary of the reef limestone, and most of the transition zone is developed in reef limestone, which is extremely unstable and can be easily destroyed. Only the transition zone above the top boundary of reef limestone is meaningful.

References

- [1] ZHAO Huan-ting, WANG Li-rong, SONG Chao-jing. Review on freshwater lens of lime-sand island in Nanhai[J]. *Marine Science Bulletin*, 2014, 33(6): 601–610.
- [2] ZHAO Huan-ting, WANG Li-rong. Construction of airfield islands on coraller in the South China Sea Islands[J]. *Tropical Geography*, 2017, 37(5): 681–693.
- [3] ZHAO Huan-ting, SONG Chao-jing, LU Bo, et al. Contents and methods of coral reef engineering geology research[J]. *Journal of Engineering Geology*, 1997, 5(1): 21–27.

- [4] SHAN Hua-gang, WANG Ren, ZHOU Zeng-hui. Engineering geological properties of Yongshu reef in Nansha Islands[J]. *Marine Geology and Quaternary Geochronology*, 2000(3): 31–36.
- [5] ZHU Chang-qi, ZHOU Bin, LIU Hai-feng. State-of-the-art review of developments of laboratory tests on cemented calcareous soils[J]. *Rock and Soil Mechanics*, 2015, 36(2): 311–319, 324.
- [6] ZHU Chang-qi, ZHOU Bin, LIU Hai-feng. Investigation on strength and microstructure of naturally cemented calcareous soil[J]. *Rock and Soil Mechanics*, 2014, 35(6): 1655–1663.
- [7] SUN Ji-zhu, WANG Ren. Influence of confining pressure on particle breakage and shear expansion of calcareous sand[J]. *Chinese Journal of Rock Mechanics and Engineering*, 2004, 23(4): 641–644.
- [8] ZHAO Yang, ZHOU Hui, FENG Xia-ting, et al. Residual shear behaviour and particle crushing of an infilled joint soil under high stress[J]. *Rock and Soil Mechanics*, 2012, 33(11): 3299–3306.
- [9] ZHANG Jia-ming, JIANG Guo-sheng, WANG Ren. Research on influences of particle breakage and dilatancy on shear strength of calcareous sands[J]. *Rock and Soil Mechanics*, 2009, 30(7): 2043–2049.
- [10] SINGH V S, GUPTA C P. Groundwater in a coral island[J]. *Environmental Geology*, 1999, 37(1): 72–76.
- [11] ROTZOLL K, OKI D S. Changes of freshwater-lens thickness in basaltic Island aquifers overlain by thick coastal sediments[J]. *Hydrogeology Journal*, 2010, 18: 1425–1436.
- [12] ZHANG Q, RAYE V, LOCKINGTON D A. Advances in environmental research[J]. *Advances in Environmental Research*, 2002, 6: 229–237.
- [13] FANG Zhen. Numerical simulation and development strategy of freshwater lens in coral reef[J]. *Southwest Water and Wastewater*, 2000(3): 31–33.
- [14] ZHOU Cong-zhi, FANG Zhen-dong, WEI Ying, et al. Exploitation and utilization of freshwater lens on coral reef islands[M]. Chongqing: Chongqing University Press, 2017.
- [15] ZHONG Jin-liang, CHEN Xin-shu, ZHANG Qiao-min, et al. Nansha Islands coral reef landform research[M]. Beijing: Science Press, 1996.
- [16] Ministry of Construction, People's Republic of China. GB 50021 - 2001 Code for investigation of geotechnical engineering(2009 edition)[S]. Beijing: China Building Industry Press, 2009.
- [17] ZHU Xu. Research on the formation of phreatic surface in an artificial coral reef island[D]. Xuzhou: China University of Mining and Technology, 2019.
- [18] The Multidisciplinary Oceanographic Expedition Team of Academia Sinica to Nansha Islands. Physical geography of Nansha islands[M]. Beijing: Science Press, 1996.
- [19] SHENG C, HAN D M, XU H H, et al. Evaluating dynamic mechanisms and formation process of freshwater lenses on reclaimed atoll islands in the South China Sea[J]. *Journal of Hydrology*, 2020, 584.
- [20] DONG Gui-ming, TIAN Juan. Numerical simulation of groundwater flow movement and pollutant migration: application analysis and practice of Visual Modflow[M]. Xuzhou: China University of Mining and Technology Press, 2013.